Translational Oncology
www.transonc.com

Volume 8 Number 2 April 2015 pp. 119–125 119

Significance of Lymph Node Metastasis in Cancer Dissemination of Head and Neck Cancer[1]

Jae-Keun Cho*,[2], Seung Hyup Hyun†,[2], Nayeon Choi‡, Min-Ji Kim§, Timothy P. Padera¶, Joon Young Choi† and Han-Sin Jeong‡

*Department of Otorhinolaryngology-Head and Neck Surgery, Pusan National University, Pusan, Korea; †Department of Nuclear Medicine, Samsung Medical Center, Sungkyunkwan University School of Medicine, Seoul, Korea; ‡Department of Otorhinolaryngology-Head and Neck Surgery, Samsung Medical Center, Sungkyunkwan University School of Medicine, Seoul, Korea; §Biostatistics and Clinical Epidemiology Center, Research Institute for Future Medicine, Samsung Medical Center, Seoul, Korea; ¶Edwin L. Steele Laboratory, Department of Radiation Oncology, Massachusetts General Hospital and Harvard Medical School, Boston, MA, USA

Abstract

Lymph node metastasis (LNM) in many solid cancers is a well-known prognostic factor; however, it has been debated whether regional LNM simply reflects tumor aggressiveness or is a source for further tumor dissemination. Similarly, the metastatic process in head and neck cancer (HNC) has not been fully evaluated. Thus, we aimed to investigate the relative significance of LNM in metastatic cascade of HNC using functional imaging of HNC patients and molecular imaging in *in vivo* models. First, we analyzed ^{18}Fluorodeoxyglucose positron emission tomography (PET) parameters of 117 patients with oral cancer. The primary tumor and nodal PET parameters were measured separately, and survival analyses were conducted on the basis of clinical and PET variables to identify significant prognostic factors. In multivariate analyses, we found that only the metastatic node PET values were significant. Next, we compared the relative frequency of lung metastasis in primary ear tumors *versus* lymph node (LN) tumors, and we tested the rate of lung metastasis in another animal model, in which each animal had both primary and LN tumors that were expressing different colors. As a result, LN tumors showed higher frequencies of lung metastasis compared to orthotopic primary tumors. In color-matched comparisons, the relative contribution to lung metastasis was higher in LN tumors than in primary tumors, although both primary and LN tumors caused lung metastases. In summary, tumors growing in the LN microenvironment spread to systemic sites more commonly than primary tumors in HNC, suggesting that the adequate management of LNM can reduce further systemic metastasis.

Translational Oncology (2015) 8, 119–125

Address all correspondence to: Han-Sin Jeong, MD, Department of Otorhinolaryngology-Head and Neck Surgery, Samsung Medical Center, Sungkyunkwan University School of Medicine, 81 Irwon-ro, Gangnam-gu, Seoul 135-710, Korea or Joon Young Choi, Department of Nuclear Medicine, Samsung Medical Center, Sungkyunkwan University School of Medicine, 81 Irwon-ro, Gangnam-gu, Seoul 135-710, Korea.
E-mail: hansin.jeong@gmail.com

[1]This work was supported by Samsung Medical Center, Research Development grant no. GL1-B2-291-1, National Research Foundation of Korea (NRF) grant funded by the Korea government (MEST) no. 2012R1A1A2040866, KIST-SMC Translational Research Project 2013 and US NIH DP2 OD008780. Conflicts of interest statement: The authors declare no conflict of interest.

[2]These authors contributed equally to this work.

Received 4 November 2014; Revised 5 March 2015; Accepted 9 March 2015

1936-5233/15
http://dx.doi.org/10.1016/j.tranon.2015.03.001

Introduction

Lymph node metastasis (LNM) in many solid cancers including head and neck cancer (HNC) is a well-known and clinically accepted prognostic factor [1,2]. However, it has been debated whether LNM reflects tumor aggressiveness or invasiveness or is a foothold for further tumor dissemination [3]. The early concept of a metastatic cascade in solid cancers was the sequential progress of tumors from the primary sites to lymph nodes (LNs) and then systemically distant organs (Halstedian theory) [4,5]. In contrast, the systemic theory of cancer metastasis highlighted the view that cancer is a systemic disease, and cancer cells disperse throughout the body at the very early phase of tumor formation [6,7]. According to this theory, the status of LNM only provides prognostic information; therefore, surgical removal of metastatic nodes does not affect patient survival. However, many clinical observations of breast [8], stomach [9], endometrial [10], and esophageal cancers [11] have not fit well into these two categories, and a spectrum theory was proposed explaining that tumor cells gain more metastatic capabilities as the tumor progresses to regional LNs [3,12] (Figure S1). Halstedian theory does not accept the direct dissemination of tumor from primary tumor to systemic sites [5]; however, the spectrum theory describes systemic tumor dissemination both from primary tumors and LNM but supposes that tumor cells spread more to systemic sites from LNM, which can be a major source of systemic disease [3].

In HNC, there have been no clear data, but similarly the active control of regional as well as local diseases is recommended for better survival of HNC patients [National Comprehensive Cancer Network (NCCN) Clinical Practice Guideline in Oncology, Head and Neck Cancer, Version 2.2013]. Molecular and genetic characteristics of cancer cells can be the main determinants of metastasis in HNC [13], and the active dissemination to blood and lymphatic vessels in the primary tumor was suggested [7]. However, the relative significance of the established LNM in further cancer dissemination of HNC has never been studied fully.

Regional LNM is a major prognostic factor for HNC, because it indicates aggressive tumor biology, as well as represents a source of subsequent metastasis (as explained by the spectrum theory) [3,14]. In addition, the tumor biology and phenotype within the primary site microenvironment can differ from those of the metastatic LNs [15–17]. More importantly, tumor cells in different microenvironments have been reported to respond differently to therapy [17–19]. Thus, increasing evidence indicates that to determine optimal treatment and to better predict prognosis, evaluation of cancer patients should be refined on the basis of the primary tumor and metastatic microenvironment.

Despite this body of knowledge, the significance of LNM and LN microenvironment has not been evaluated. Thus, the aims of this study were to provide clinical and experimental evidence regarding the role of established LNM in the metastatic cascade of HNC by analyzing functional imaging in HNC patients and using molecular imaging in *in vivo* models. Understanding metastasis progression of HNC in tumor site–specific microenvironments can lead to personalized treatments and refine the design of many clinical trials enrolling patients with metastatic/recurrent HNC.

Materials and Methods

Evaluation of ^{18}F-FDG PET/CT Imaging in Oral Cancer Patients

First, we evaluated the ^{18}Fluorodeoxyglucose positron emission tomography (18F-FDG PET)/computed tomography (CT) imaging in HNC patients. Our study population was limited to oral cavity squamous cell carcinoma patients, because the standard treatment is initial surgery and/or post-operative adjuvant treatment, which enabled us to access pathologic information. Newly diagnosed oral cavity cancer patients were prospectively enrolled in the study from 2006 to 2012. All participants provided written informed consent before the study. The diagnosis of oral cavity squamous cell carcinoma was confirmed by surgical pathology in all subjects. Patients with other pathology types, uncontrolled diabetes, or high blood glucose level (>200 mg/dl), secondary malignancies, or who failed to receive definitive treatment for disease were excluded from the analyses (N = 20). Finally, 117 patients were included in this study. All patients were subjected to curative resection of the primary tumor with neck LN dissection (N = 71) or sentinel LN biopsy (N = 46). The demographics and clinicopathologic characteristics of the patients are summarized in Table S1. Whole-body ^{18}F-FDG PET and unenhanced CT images were acquired using integrated PET/CT scanners according to the standard protocols (Discovery LS or Discovery STE; GE Healthcare, Pittsburgh, PA).

Measurement of ^{18}F-FDG PET Variables

^{18}F-FDG PET measurements were performed using the Volume Viewer software on the GE Advantage Workstation version 4.4 (GE Healthcare). This software automatically determines the volume of interest using an iso-contour threshold method based on the standardized uptake value (SUV). The volumes of interest were placed over the target lesions within the primary sites as well as all suspicious metastatic LNs, and the software subsequently measured the maximum SUV (SUV_{max}), average SUV, and metabolic tumor volume (MTV). The MTV represents a volumetric measurement of tumor cells with high glycolytic activity and was defined as the tumor volume segmented with ^{18}F-FDG uptake above a threshold SUV of 2.5. We measured the SUV_{max} and MTV of the primary tumor ($pSUV_{max}$ and pMTV) and metastatic LN ($nSUV_{max}$ and nMTV) on the pretreatment scan. We also calculated total lesion glycolysis (TLG) as the product of MTV and average SUV in both the primary tumor (pTLG) and metastatic LN (nTLG). In multiple metastatic nodes, $nSUV_{max}$ reflected the highest SUV among metastatic nodes, whereas nMTV and nTLG indicated the sum of all nodes.

If the target lesion was not visualized or could not be distinguished from background, SUV_{max} and MTV values were set as zero. When the target lesion was visible but the SUV_{max} was less than 2.5, the MTV was set as a single voxel with a volume of 0.05 cm^3.

Statistical Analyses

To estimate the predictive performance of ^{18}F-FDG PET parameters, for time-to- event data, we used time-dependent receiver operating characteristic (ROC) curve [20–22]. ^{18}F-FDG PET parameters were stratified using optimal cutoff values based on the highest Youden's index from time-dependent ROC curves at 24 months [23]. Univariate and multivariate analyses of pretreatment variables were conducted using a Cox proportional hazards regression model to identify significant variables for disease-free survival (DFS) and overall survival (OS). Statistical analyses were performed using SAS version 9.3 (SAS Institute, Cary, NC) and R 2.13.2 (Vienna, Austria; http://www.R-project.org/). Time-dependent ROC curves were determined using the "survival ROC" package for R [21]. All tests were two-sided, and P values <.05 were considered statistically significant.

Table 1. Univariate Analyses for Survival Analyses of Clinical and PET Variables for Oral Cancer Patient Survival

Pretreatment Variables	DFS			OS		
	HR	95% CI	*P*	HR	95% CI	*P*
Age (1-year increase)	1.002	0.975-1.030	.888	1.020	0.983-1.059	.283
Gender (M *vs* F)	1.094	0.484-2.474	.828	1.065	0.375-3.027	.905
Clinical T classification						
T3-4 *vs* T1-2	3.907	1.835-8.320	<.001	2.969	1.097-8.035	.032
Clinical N classification						
N1-2 *vs* N0	1.708	0.821-3.554	.152	3.391	1.194-9.629	.022
^{18}F-FDG PET measurements†						
$pSUV_{max}$	3.862	1.648-9.049	.002	2.861	1.008-8.123	.048
pMTV	2.477	1.151-5.329	.020	1.866	0.710-4.906	.206
pTLG	2.881	1.276-6.508	.011	2.161	0.833-5.602	.113
$nSUV_{max}$	2.872	1.307-6.314	.009	5.444	2.097-14.134	<.001
nMTV	3.071	1.397-6.752	.005	4.428	1.684-11.642	.003
nTLG	2.978	1.355-6.547	.007	4.902	1.597-15.045	.006

HR, hazard ratio; CI, confidence interval; p, primary tumor; n, metastatic node.
Analyses conducted using Cox proportional hazard model.
† PET values were dichotomized using the optimal cutoff values.

Table 2. Multivariate Analysis of Clinical and PET Variables for Oral Cancer Patient Survival

Pretreatment variables	DFS			OS		
	HR	95% CI	*P*	HR	95% CI	*P*
SUV_{max} model						
Clinical T (T3-4 *vs* T1-2)	2.457	1.081-5.581	.032	2.101	0.691-6.389	.191
Clinical N (N1-2 *vs* N0)	0.526	0.187-1.477	.223	1.476	0.378-5.757	.575
$pSUV_{max}$	2.414	0.897-6.500	.081	1.392	0.403-4.811	.601
$nSUV_{max}$	3.182	1.094-9.254	.034	3.621	1.085-12.088	.036
MTV model						
Clinical T (T3-4 *vs* T1-2)	2.882	1.230-6.753	.015	2.905	0.943-8.954	.063
Clinical N (N1-2 *vs* N0)	0.627	0.240-1.639	.341	1.460	0.348-6.131	.605
pMTV	1.357	0.563-3.269	.496	0.740	0.240-2.279	.600
nMTV	3.529	1.256-9.914	.017	3.486	0.898-13.526	.071
TLG model						
Clinical T (T3-4 *vs* T1-2)	2.782	1.226-6.309	.014	3.065	0.752-12.491	.118
Clinical N (N1-2 *vs* N0)	0.615	0.233-1.621	.325	1.270	0.311-5.182	.739
pTLG	1.643	0.664-4.064	.282	0.696	0.173-2.795	.609
nTLG	3.358	1.180-9556	.023	4.122	0.872-19.483	.074

Analyses conducted using Cox proportional hazard model; p, primary tumor; n, metastatic node.

Comparison of Systemic Metastasis from Primary Tumors and LN Tumors

All animal experiment protocols were approved by the Institutional Committee for Laboratory Animal Research. First, we tested which tumors in primary sites *versus* in LNs spread more frequently to distant organs. The SCCVII cells we used were cutaneous, moderately differentiated, murine squamous cell carcinomas, syngeneic to C3H mice, which had originally been isolated and cultured by Dr Herman D. Suit (Harvard Medical School, Radiation Oncology).

To compare the occurrence of lung metastasis between primary and LN tumors, we directly injected SCCVII tumor cells into the parotid/upper cervical LN of C3H/HeJ mice (female, 6 weeks) using a Hamilton syringe ($1\text{-}5 \times 10^4$ cells in 1 μl; $N = 13$). Then, we compared the occurrence of lung metastasis in these animals with that in animals with ear tumors ($N = 14$). When the animals started losing body weight (>10%), they were sacrificed and the tumors were collected. The tumor volumes at the end point did not differ between the two groups (ear tumor: 288 ± 42 mm^3, LN tumor: 312 ± 40 mm^3), and the time period until the possible occurrence of lung metastasis (loss of body weight) was 7 weeks (median) with a range of 5 to 12 weeks. For the control group ($N = 8$), we removed the LN immediately after tumor cell injection to exclude any possible effects of tumor cell leakage or direct systemic dissemination due to the injection procedure.

Evaluation of Systemic Metastasis in Animals with Both Primary and LN Tumors

Next, we created a clinically relevant animal model, in which each animal had both primary and LN tumors. To differentiate between these two tumors in the same mouse, we generated tumor cells expressing either green fluorescence (SCCVII-GFP) or dual colors (SCCVII-dsRed/GFP) and injected the tumor cells into the ear (5×10^5 cells in 100 μl) and the draining LN ($1\text{-}5 \times 10^4$ cells in 1 μl) simultaneously. When mice started losing body weight (>10%), they were sacrificed and the tumors were collected. The tumors were evaluated using fluorescent microscopy to determine the color expressed within each metastatic tumor. We considered that the color of the metastatic tumors identified the source tumor from which it originated (ear or LN tumor). The "unit metastasis potential" of the primary or LN tumor was calculated as the tumor volume and number of lung metastases divided by the original tumor volume. To exclude any difference of metastatic potential between SCCVII-GFP and SCCVII-dsRed/GFP cells, we conducted two sets of experiments in which the injection of the different colored tumor cells was switched between the ear and LN ($N = 11$ and 8).

Results

PET Measurements of Metastatic LNs Have a Higher Diagnostic Performance to Discriminate Survival Status

^{18}F-FDG PET/CT correctly diagnosed 37 of 52 patients (71.2%) with clinical neck metastases and 58 of 65 (89.2%) subjects without neck metastases based on surgical pathology. These findings were consistent with the previous study reporting that PET imaging does not have high diagnostic performance to detect occult nodal metastases [24].

To determine the best cutoff values for discriminating survival status, we calculated Youden's index (= sensitivity + specificity − 1) (Table S2). We found a significantly better discrimination of DFS status using $nSUV_{max}$ than using $pSUV_{max}$ ($P = .045$), suggesting that nodal ^{18}F-FDG PET measurements are better predictors of DFS compared to the primary tumor. Similarly, we set the following cutoff values for the best discrimination of OS status at 24 months. The area under the curve from the time-dependent ROC curve analysis at 24 months was approximately 0.60 to 0.81, and there was no significant difference in the discriminative power between primary tumor and metastatic nodal ^{18}F- FDG PET measurements in terms of OS.

PET Values of Metastatic LN Correlate with Prognosis Better than Primary Tumor PET Values in Oral Cancer

We conducted survival analyses using clinical variables and ^{18}F-FDG PET values to identify prognostic factors that significantly affect survival. Because we were concerned with the clinical decision-making and prognosis before any treatment initiation, we included only the clinical variables as possible prognostic factors, along with PET values. Univariate analysis indicated that clinical T classification and all ^{18}F-FDG PET values were significant prognostic factors for DFS and that clinical T and N classifications, $pSUV_{max}$, $nSUV_{max}$, nMTV, and nTLG were significant for OS (Table 1).

In the multivariate analyses, we excluded the variables that did not reach statistical significance in univariate survival analyses (age and gender) and included clinical T and N classifications and ^{18}F-FDG PET values. We rendered three separate multivariate models based on

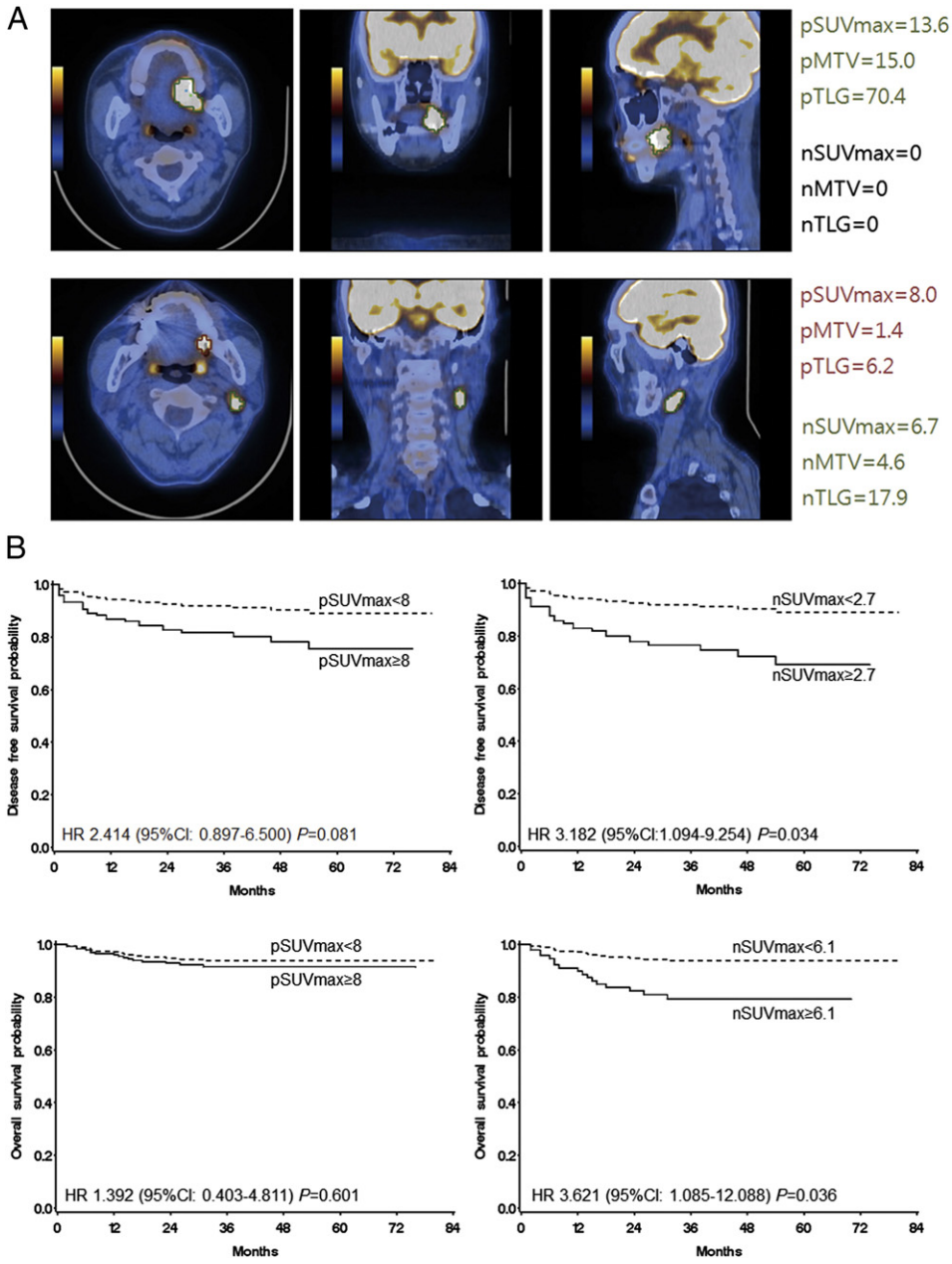

Figure 1. Survival plots according to primary tumor and metastatic node ^{18}F-FDG PET values. (A) Representative cases: This patient had T2 tongue cancer but no LNM (upper), whereas the other patient had small T1 tongue cancer with an ipsilateral LNM (lower). We measured ^{18}F-FDG PET values of primary tumor and LNM, separately using automatic volume calculation software with a threshold SUV of 2.5. (B) Curves were estimated by the Cox proportional hazard model for multivariate analyses. DFS and OS were presented according to the dichotomized $pSUV_{max}$ and $nSUV_{max}$ values, and these curves represented the relative survivals of two groups with other possible factors adjusted. p, primary tumor; n, metastatic node.

SUV_{max} and volume-based ^{18}F-FDG PET values (MTV and TLG), because significant multi-collinearity existed among the ^{18}F-FDG PET measurements (variation inflation factor > 10). Regarding DFS, the three multivariate models indicated that clinical T classification and metastatic LN ^{18}F-FDG PET values ($nSUV_{max}$, nMTV, and nTLG) were significant risk factors (Table 2). In OS analyses, only the metastatic LN $nSUV_{max}$ showed statistical significance (Figure 1).

In addition, we found 15 distant metastases in our series during follow-up: 1 in pN0, 3 in pN1 and 11 in pN2 (pN0 *vs* pN1-2, $P <$ .001). There were 12 distant metastasis in high $nSUV_{max}$ (≥2.7) and 3 in low $nSUV_{max}$ (<2.7; P = .008).

LN Tumors Show a Higher Frequency of Lung Metastasis than Primary Tumors in In Vivo Animal Models

LN tumors were formed by direct injection of tumor cells into the LN, which solely reflected tumor growth of the same cancer cells in different microenvironments. Tumors in the LN caused significantly more and larger lung metastases than did primary ear tumors in tumor volume–matched comparison (Figure 2).

One of eight animals in the control group (mice that underwent immediate removal of the LN after tumor cell injection) showed lung metastases, and three of eight mice had tumor formation in the surrounding LN, suggesting that tumor cell leakages occurred during

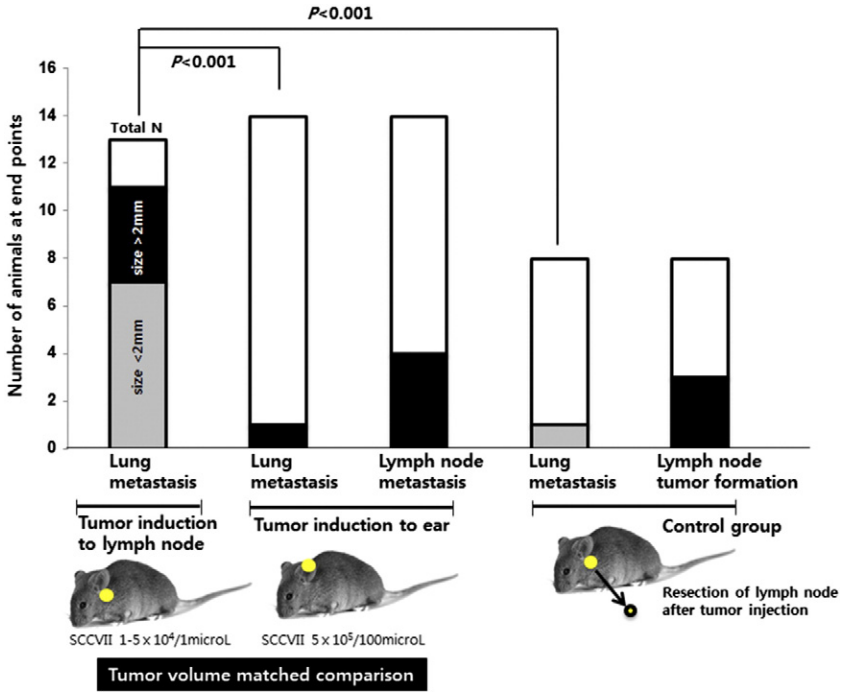

Figure 2. Comparison of systemic metastasis from primary tumors and LN tumors. For LN tumor induction, tumor cells (SCCVII, 1-5 $\times$ 10^4 cells in 1 μl) were directly injected into the parotid/upper cervical LN of C3H/HeJ animals using a Hamilton syringe (N = 13). Ear tumors were induced by injecting tumor cells (5 $\times$ 10^5 cells in 100 μl) into the ear (N = 14). When the animals started to lose body weights (>10%), they were sacrificed and the occurrence of lung metastasis was compared between two groups. In the control group, we removed the LN immediately after tumor cell injection into the LN (N = 8).

the tumor cell injection into the LN. Thus, the increase in size and number of lung metastases from tumors implanted directly in the LN, compared to those from primary ear tumors, may come from technical factors as well as differential tumor microenvironments (soil). Considering the magnitude of lung metastasis, the tumors established in the LN had a relatively high tendency of more lung metastasis compared with those in the primary site (ear).

LN Tumors Have Higher Systemic Metastatic Capabilities than Primary Tumors

Next, we evaluated the relative contribution of primary and LN tumors to systemic metastasis in an animal model having both tumors of different colors simultaneously, similar to what a locally advanced HNC patient might have. We calculated the original tumor volumes of ear and LN tumors as well as the total volume or numbers of lung metastasis nodules. After the tumor volume and number of lung nodules were divided by the original color-matched tumor volume (defined as the unit metastasis potentials), the calculated LN tumor values were found to be significantly greater than the primary tumor values (Figure 3). The difference was large, even considering tumor cell leakage during the LN injection procedure. Thus, these results suggest that a greater degree of systemic metastasis occurred from established LN tumors compared to primary tumors.

Discussion

LNM in many solid cancers including HNC is a well-known and clinically accepted prognostic factor [1,2]. However, the significance of LNM has been debated for decades [3]. Here, we demonstrated that there is more systemic spread from established LN tumors than from primary tumors in preclinical animal models. In addition, in oral cancer patients, we found that metabolic measurements of regional metastatic LN correlated with patient DFS better than those of primary tumors. Thus, our data support the significance of LNM in HNC, which can be the potential major source of further systemic metastasis [3].

This report is the first to provide direct clinical and experimental evidence of LNM as a source of further cancer spread. Despite LNM being as a strong prognostic factor for recurrence and survival, few previous investigations regarding the significance of metastatic LNs have been performed. Clinically, it is difficult to determine the tumor origin from which systemic metastasis is derived. To overcome this limitation and validate clinical findings of nodal metabolic significance, we conducted two *in vivo* animal studies to evaluate the relative impact of primary *versus* LN tumors on systemic metastasis. We confirmed higher metastatic potential in established LN tumors, which is in accordance with the clinical findings. Tumor cells growing within the LN microenvironment, compared with the same tumor cells growing in its primary site, showed a higher frequency of lung metastasis, suggesting a role of the unique LN microenvironment in the formation of systemic metastasis.

Still, the OS of HNC patients has not significantly improved despite improved loco-regional control [25–28]. On the basis of our data that proved a high risk of systemic metastasis from LNM in HNC, it suggests some therapeutic implications to improve the OS in HNC patients. Adjuvant systemic treatments that prevent the clinical and fatal systemic diseases from circulating tumor cells [29,30] or distant micro-metastasis [7] could be incorporated into the multimodality treatment protocols particularly in HNC patients with a large burden of nodal diseases.

It is important to note the difference in tumor biology between the primary site and LNs. We found that the metastatic capability of tumor cells depended on the tumor microenvironment, because there was no selection process of tumor cells in our study. Recent data also indicated that the biology of the primary tumor differs from that of the metastatic LNs [15–17], and importantly, tumor cells in different microenvironments

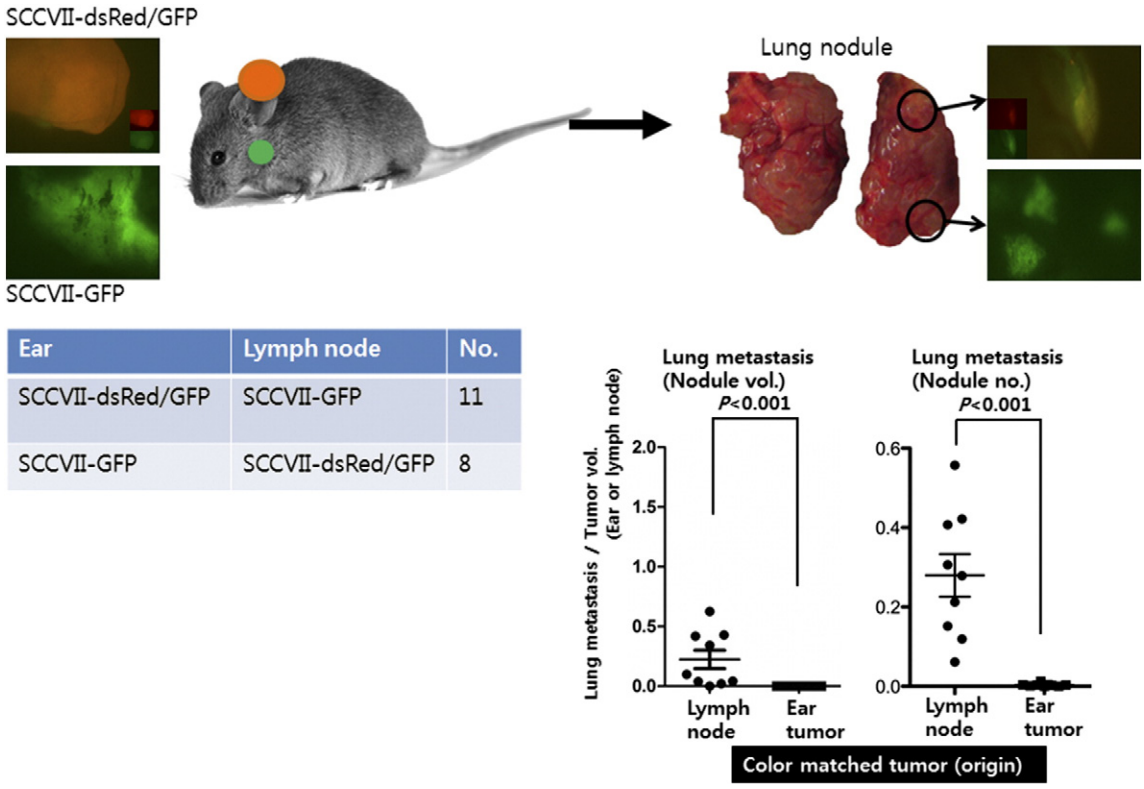

Figure 3. Relative risk of systemic metastasis from primary and LN tumors. (A) To differentiate two tumors in the same mouse, we simultaneously induced different colored tumors into the ear (5×10^5 cells in 100 μl) and the draining LN ($1\text{-}5 \times 10^4$ cells in 1 μl): SCCVII-GFP into the ear and SCCVII-dsRed/GFP into the LN and *vice versa*. When the animals started to lose body weight (>10%), animals were sacrificed and tumors were evaluated using fluorescent microscopy to determine the color of each metastasis. (B) To exclude any difference in metastatic potential between SCCVII-GFP and SCCVII-dsRed/GFP cells, we conducted two sets of experiments in which the injection of the different colored tumor cells was switched between the ear and LN ($N = 11$ and 8). (C) We considered the color-matched metastatic tumors as originating from the same color implanted tumor (ear or LN tumor). We calculated the unit metastasis potential of the original tumors, defined as tumor volume or number of lung metastasis divided by the original tumor volume.

respond differently to therapy [17–19]. Unfortunately, most studies of tumor biology, drug response, and clinical trials do not evaluate the setting of nodal metastasis. Thus, understanding tumor biology in each metastatic site and evaluation of cancer based on the tumor and specific metastatic microenvironment would help determine the optimal treatment protocol and better predict prognosis.

However, our study had some limitations. Our *in vivo* models were manipulated such that the possibility of tumor selection was completely excluded, which may not reflect the real LNM from primary tumors. Nevertheless, we could observe solely the differential impacts on tumor dissemination of primary tumor sites and LNs without confounding of tumor cell properties using our *in vivo* models. So, we think our models were best fit for studying the sole impact of tumor microenvironments (soil), although they were very artificial. In addition, ear tumor models probably did not reflect well the oral cavity cancer in human, where ear tumors have less lymphatic vessels than oral cavity tumors. However, we focused on each tumor growing in the primary sites or LNs, not on the intervening lymphatics between them. If there were profuse lymphatics in the primary sites, it is likely to have more lymphatic metastasis from primary tumors.

In addition, we measured the rate and occurrence of lung metastasis at only one time point. Thus, we cannot make any conclusions about systemic spread over time from primary and LN tumors. Moreover, the precise route leading into systemic circulation was not determined in this study and requires further mechanistic investigation. However, one suggestion is the extracapsular spread of LNM and extranodal blood vessels [31]. In clinical data, the volumetric values of LNM appeared to be subject to a wide range of measurement errors, perhaps due to the relatively small tumor volume of metastatic node in the limited N disease cases (N1). Another thing to note is that our clinical study proved the significance of LNM in HNC patients, not providing the direct evidence of systemic dissemination from LN tumors. Thus, one should keep in mind that the formation of vital organ metastasis may be a complex process contributed by intrinsic cancer cell properties, tumor microenvironments, and their interactions. Nevertheless, we confirmed a strong correlation between $nSUV_{max}$ and patient survival. Finally, the study subjects were limited to oral cancer patients, where surgical pathology was available. Thus, our results require future validation in other types of HNC.

Tumor-Node-Metastasis (TNM) staging, which is currently the best predictor of patient prognosis and the determinants of the treatment method, simultaneously takes into account the primary tumor dimension and LNM status. However, high T (T3-4), low N (N0-1) stage and low T (T1-2), high N (N2-3) stage tumors are classified into the same TNM staging category in HNC. In addition, a variety of non-surgical treatment options leave pathologic T and N status unknown. According to our current data, metabolic nodal imaging can be used as an additional tool to provide pretreatment prognostic biomarkers and risk stratification, along with the clinical TNM stage, because metabolic PET parameters can reflect well the pathologic status (Table S3).

Conclusion

In summary, the present study provided clinical and experimental data regarding the significance of LNM in HNC and supported the spectrum theory of tumor metastasis, where tumor cells gain more metastatic capabilities as the tumor progresses to regional LNs in HNC.

Appendix A. . Supplementary data

Supplementary data to this article can be found online at http://dx.doi.org/10.1016/j.tranon.2015.03.001.

References

[1] Gil Z, Carlson DL, Boyle JO, Kraus DH, Shah JP, Shaha AR, Singh B, Wong RJ, and Patel SG (2009). Lymph node density is a significant predictor of outcome in patients with oral cancer. *Cancer* **115**, 5700–5710.

[2] Kowalski LP, Bagietto R, Lara JR, Santos RL, Silva Jr JF, and Magrin J (2000). Prognostic significance of the distribution of neck node metastasis from oral carcinoma. *Head Neck* **22**, 207–214.

[3] Kawada K and Taketo MM (2011). Significance and mechanism of lymph node metastasis in cancer progression. *Cancer Res* **71**, 1214–1218.

[4] Crile G (1987). Landmark article Dec 1, 1906: Excision of cancer of the head and neck. With special reference to the plan of dissection based on one hundred and thirty-two operations. By George Crile. *JAMA* **258**, 3286–3293.

[5] Halsted WS (1907). I. The results of radical operations for the cure of carcinoma of the breast. *Ann Surg* **46**, 1–19.

[6] Fisher B (1980). Laboratory and clinical research in breast cancer—a personal adventure: the David A. Karnofsky memorial lecture. *Cancer Res* **40**, 3863–3874.

[7] Allen CT, Law JH, Dunn GP, and Uppaluri R (2013). Emerging insights into head and neck cancer metastasis. *Head Neck* **35**, 1669–1678.

[8] Clarke M, Collins R, Darby S, Davies C, Elphinstone P, Evans E, Godwin J, Gray R, Hicks C, and James S, et al (2005). Effects of radiotherapy and of differences in the extent of surgery for early breast cancer on local recurrence and 15-year survival: an overview of the randomised trials. *Lancet* **366**, 2087–2106.

[9] Wu CW, Hsiung CA, Lo SS, Hsieh MC, Chen JH, Li AF, Lui WY, and Whang-Peng J (2006). Nodal dissection for patients with gastric cancer: a randomised controlled trial. *Lancet Oncol* **7**, 309–315.

[10] Todo Y, Kato H, Kaneuchi M, Watari H, Takeda M, and Sakuragi N (2010). Survival effect of para-aortic lymphadenectomy in endometrial cancer (SEPAL study): a retrospective cohort analysis. *Lancet* **375**, 1165–1172.

[11] Jamieson GG, Lamb PJ, and Thompson SK (2009). The role of lymphadenectomy in esophageal cancer. *Ann Surg* **250**, 206–209.

[12] Hellman S (1994). Karnofsky Memorial Lecture. Natural history of small breast cancers. *J Clin Oncol* **12**, 2229–2234.

[13] Timar J, Csuka O, Remenar E, Repassy G, and Kasler M (2005). Progression of head and neck squamous cell cancer. *Cancer Metastasis Rev* **24**, 107–127.

[14] Datta K, Muders M, Zhang H, and Tindall DJ (2010). Mechanism of lymph node metastasis in prostate cancer. *Future Oncol* **6**, 823–836.

[15] Akita H, Doki Y, Yano M, Miyata H, Miyashiro I, Ohigashi H, Ishikawa O, Nishiyama A, and Imaoka S (2009). Effects of neoadjuvant chemotherapy on primary tumor and lymph node metastasis in esophageal squamous cell carcinoma: additive association with prognosis. *Dis Esophagus* **22**, 291–297.

[16] Falck AK, Ferno M, Bendahl PO, and Ryden L (2013). St Gallen molecular subtypes in primary breast cancer and matched lymph node metastases—aspects on distribution and prognosis for patients with luminal A tumours: results from a prospective randomised trial. *BMC Cancer* **13**, 558.

[17] Fruhwirth GO, Diocou S, Blower PJ, Ng T, and Mullen GE (2014). A whole-body dual-modality radionuclide optical strategy for preclinical imaging of metastasis and heterogeneous treatment response in different microenvironments. *J Nucl Med* **55**, 686–694.

[18] Padera TP, Kuo AH, Hoshida T, Liao S, Lobo J, Kozak KR, Fukumura D, and Jain RK (2008). Differential response of primary tumor versus lymphatic metastasis to VEGFR-2 and VEGFR-3 kinase inhibitors cediranib and vandetanib. *Mol Cancer Ther* **7**, 2272–2279.

[19] Medich D, McGinty J, Parda D, Karlovits S, Davis C, Caushaj P, and Lembersky B (2001). Preoperative chemoradiotherapy and radical surgery for locally advanced distal rectal adenocarcinoma: pathologic findings and clinical implications. *Dis Colon Rectum* **44**, 1123–1128.

[20] Haibe-Kains B, Desmedt C, Sotiriou C, and Bontempi G (2008). A comparative study of survival models for breast cancer prognostication based on microarray data: does a single gene beat them all? *Bioinformatics* **24**, 2200–2208.

[21] Heagerty PJ, Lumley T, and Pepe MS (2000). Time-dependent ROC curves for censored survival data and a diagnostic marker. *Biometrics* **56**, 337–344.

[22] Schmid M and Potapov S (2012). A comparison of estimators to evaluate the discriminatory power of time-to-event models. *Stat Med* **31**, 2588–2609.

[23] Youden WJ (1950). Index for rating diagnostic tests. *Cancer* **3**, 32–35.

[24] Kyzas PA, Evangelou E, Denaxa-Kyza D, and Ioannidis JP (2008). ^{18}F-fluorodeoxyglucose positron emission tomography to evaluate cervical node metastases in patients with head and neck squamous cell carcinoma: a meta-analysis. *J Natl Cancer Inst* **100**, 712–720.

[25] Seiwert TY and Cohen EE (2005). State-of-the-art management of locally advanced head and neck cancer. *Br J Cancer* **92**, 1341–1348.

[26] Michiels S, Le Maitre A, Buyse M, Burzykowski T, Maillard E, Bogaerts J, Vermorken JB, Budach W, Pajak TF, and Ang KK, et al (2009). Surrogate endpoints for overall survival in locally advanced head and neck cancer: meta-analyses of individual patient data. *Lancet Oncol* **10**, 341–350.

[27] Genden EM, Ferlito A, Bradley PJ, Rinaldo A, and Scully C (2003). Neck disease and distant metastases. *Oral Oncol* **39**, 207–212.

[28] Yao M, Lu M, Savvides PS, Rezaee R, Zender CA, Lavertu P, Buatti JM, and Machtay M (2012). Distant metastases in head-and-neck squamous cell carcinoma treated with intensity-modulated radiotherapy. *Int J Radiat Oncol Biol Phys* **83**, 684–689.

[29] Nichols AC, Lowes LE, Szeto CC, Basmaji J, Dhaliwal S, Chapeskie C, Todorovic B, Read N, Venkatesan V, and Hammond A, et al (2012). Detection of circulating tumor cells in advanced head and neck cancer using the CellSearch system. *Head Neck* **34**, 1440–1444.

[30] Jatana KR, Balasubramanian P, Lang JC, Yang L, Jatana CA, White E, Agrawal A, Ozer E, Schuller DE, and Teknos TN, et al (2010). Significance of circulating tumor cells in patients with squamous cell carcinoma of the head and neck: initial results. *Arch Otolaryngol Head Neck Surg* **136**, 1274–1279.

[31] Lee WY, Shin DY, Kim HJ, Ko YH, Kim S, and Jeong HS (2014). Prognostic significance of epithelial-mesenchymal transition of extracapsular spread tumors in lymph node metastases of head and neck cancer. *Ann Surg Oncol* **21**, 1904–1911.